

***Final Draft***  
**of the original manuscript:**

Pyczak, F.; Bauer, A.; Goeken, M.; Neumeier, S.; Lorenz, U.; Oehring, M.;  
Schell, N.; Schreyer, A.; Stark, A.; Symanzik, F.

**Plastic deformation mechanisms in a crept L12 hardened  
Co-base superalloy**

In: Materials Science and Engineering A (2013) Elsevier

DOI: 10.1016/j.msea.2013.02.007

# Plastic Deformation Mechanisms in a Crept L1<sub>2</sub> hardened Co-Base Superalloy

F. Pyczak\*<sup>1</sup>, A. Bauer<sup>2</sup>, M. Göken<sup>2</sup>, S. Neumeier<sup>2</sup>, U. Lorenz<sup>1</sup>, M. Oehring<sup>1</sup>, N. Schell<sup>1</sup>, A. Schreyer<sup>1</sup>, A. Stark<sup>1</sup>, F. Symanzik<sup>3</sup>

<sup>1</sup>Helmholtz-Zentrum Geesthacht, Centre for Materials and Coastal Research, 21502 Geesthacht, Germany

<sup>2</sup>Department of Materials Science & Engineering, Institute I, University Erlangen-Nürnberg, 91058 Erlangen, Germany

<sup>3</sup>Helmut-Schmidt-University, 22008 Hamburg, Germany

\*corresponding author: Helmholtz-Zentrum Geesthacht, Max-Planck-Str. 1, D-21502 Geesthacht, Germany, tel.: +49-4152-87-2545, e-mail: florian.pyczak@hzg.de

**Keywords:** cobalt based superalloys, creep, dislocations, transmission electron microscopy, synchrotron X-ray diffraction

## Abstract

Plastic deformation mechanisms in a crept L1<sub>2</sub> hardened Co-base superalloy are investigated by transmission electron microscopy. The deformation happens mainly in the cobalt solid solution matrix by slip of ordinary  $a/2\langle 101 \rangle\{111\}$  dislocations and rafting of the  $\gamma'$  precipitates perpendicular to the external compressive stress axis is observed. Dislocation structures are early stages of the development of  $\gamma/\gamma'$  interfacial dislocation networks. Furthermore,  $\gamma'$  precipitates are sheared by partial dislocations generating stacking faults which sometimes extend over matrix channels and neighboring  $\gamma'$  precipitates. Due to the positive lattice mismatch at creep temperature the dislocation activity in matrix channels perpendicular to the compressive external stress axis is less pronounced compared to parallel channels.

## *Introduction*

The recent discovery of an ordered L1<sub>2</sub> precipitate phase in the ternary system Co-Al-W by Sato et al. [1] generated significant interest because it opens a perspective to utilize the same hardening mechanism, which works so efficiently in Ni-base superalloys, also in Co-base superalloys. This is of technological interest as these novel Co-base alloys may offer a number of advantages with respect to corrosion resistance [2,3] and castability [4,5] when compared with Ni-base superalloys. Due to the similarity of these Co-base superalloys with Ni-base superalloys with respect to microstructure, the two phases will in the following be termed  $\gamma$ -phase for the cobalt solid solution matrix and  $\gamma'$ -phase for the ordered L1<sub>2</sub> precipitates. Because L1<sub>2</sub> hardened Co-base superalloys are a relatively novel material class only few investigations about mechanical properties and the micromechanical mechanisms of deformation are available until now [6,7]. In particular only a limited number of papers [8,9,10,11] report on creep properties. But except from few preliminary results of transmission electron microscopy (TEM) investigations by some of the authors [10,12] no information about plastic deformation mechanisms during creep is reported. For compressive deformation tests at different temperatures the dislocation structure was investigated by Suzuki et al. [6,7]. They found a pronounced flow stress anomaly. The deformation in the matrix channels occurred by type  $a/2\langle 101 \rangle$  dislocations and shearing of precipitates by type  $a/3\langle 112 \rangle$  superpartials was observed quite frequently in a quaternary Co-W-Al-Ta alloy at higher temperatures by them. These superpartials stem from reactions of  $a/2\langle 101 \rangle$  dislocations either in the matrix or at the matrix-precipitate interfaces. The  $a/3\langle 112 \rangle$  superpartial generates a superintrinsic stacking fault (SISF) within the  $\gamma'$ -precipitates. In a ternary Co-Al-W alloy on the contrary no cutting of  $\gamma'$  precipitates associated with stacking faults was observed by them [7]. If similar dislocation structures and planar defects are present in crept specimens is unknown until now.

With respect to creep it is interesting to note that it was already reported by Sato et al. that the alloy Co-9.2Al-9W has a positive lattice mismatch at room temperature [1]. For Ni-base superalloys it is well known that the lattice mismatch between the phases  $\gamma$  and  $\gamma'$  has a strong influence on the development of the dislocation structure and precipitate morphology during creep. Dislocations are first generated and glide in the softer  $\gamma$ -matrix phase. As the mismatch stresses superimpose on the externally applied stress they can either facilitate or suppress dislocation

generation and movement in the matrix channels. Another effect associated with the misfit and the coherency stresses is the so called rafting. The  $\gamma'$  particles coarsen directionally in such a way that matrix channels where the externally applied stresses add up to the coherency stresses between the phases  $\gamma$  and  $\gamma'$  vanish during creep at higher temperatures. According to Nabarro [13] for  $\sigma \cdot \delta > 0$  the onset of dislocation activity takes place first in vertical matrix channels and the raft structure is oriented parallel to the external stress axis while the situation is reversed for  $\sigma \cdot \delta < 0$ . Here  $\sigma$  is the externally applied stress and  $\delta$  the lattice mismatch which is calculated by the formula:  $\delta = 2(a_{\gamma'} - a_{\gamma}) / (a_{\gamma'} + a_{\gamma})$  with  $a_{\gamma}$  and  $a_{\gamma'}$  being the lattice parameters of the phases  $\gamma$  and  $\gamma'$ . While the fact that the onset of dislocation activity can switch between different orientations of matrix channels for a change in the sign of the externally applied stress is well documented the same is not experimentally well proofed for the sign of the lattice mismatch  $\delta$ . This is mainly due to the fact that the vast majority of Ni-base superalloys have a negative lattice mismatch at temperatures where creep deformation is normally observed. While the positive lattice mismatch at room temperature reported by Sato et al. [1] is no evidence that the mismatch is also positive at creep temperature as its amount and sign can change with temperature it is interesting to note that Titus et al. recently reported [9] that rafting parallel to the external tensile stress axis occurs in some of these novel Co-based superalloys during creep. This is a clear hint that in these alloys a positive lattice mismatch is also present at creep temperature. In the present work the lattice constants of the phases  $\gamma$  and  $\gamma'$  and the resulting lattice mismatch in a Co-9Al-9W-0.1B alloy is measured by X-ray diffraction with synchrotron radiation at room and creep temperature to confirm the positive mismatch between room temperature and 900 °C. The development of the dislocation and  $\gamma/\gamma'$  structure during creep will be investigated by TEM and scanning electron microscopy (SEM) to check experimentally if the effects proposed by Nabarro [13] for a positive mismatch in Ni-base superalloys are present in this positive mismatch Co-base superalloy. To the knowledge of the authors this is the first work that experimentally investigates the dislocation structure in a positive mismatch alloy as well as the elevated temperature lattice mismatch and dislocation structures in crept novel L1<sub>2</sub> hardened Co-base superalloys.

### *Experimental*

The nominal chemical composition of the alloy under investigation was Co-9Al-9W-0.1B (all atomic %). Recently Shinagawa et al. showed that small additions of boron are beneficial for the ductility of polycrystalline Co-base superalloys [14]. This effect is mainly caused by grain boundary strengthening and boron was added to the alloy composition under investigation to benefit from it. The alloy was produced as 100 g ingot in a vacuum arc melting furnace. By energy dispersive X-ray spectroscopy in the scanning electron microscope the alloy chemistry was checked and was found to be 82.2% cobalt, 8.3% aluminium and 9.4% tungsten [8]. The content of boron cannot be determined precisely with this method and was therefore not taken into account. Subsequent to melting the ingot was solution heat treated at 1300 °C for 12 h in argon and aged at 900 °C for 200 h in air. This resulted in a  $\gamma'$ -volume fraction of 58 % [8]. It is important to note that no secondary  $\gamma'$  precipitates within the matrix channels were present in the material, while secondary  $\gamma'$  particles were found in the specimens investigated by Suzuki et al. [7]. From this heat treated ingot cylindrical specimens for creep experiments with a length of 7.5 mm and a diameter of 5 mm were produced by electro spark erosion. The creep tests were performed under compression at 850 °C and 900 °C. For TEM investigations a specimen crept at 850 °C with load increments of 250 MPa, 350 MPa and 450 MPa, which were applied subsequent to the creep minimum, was used. A plastic strain of up to 2 % was reached before the test was stopped and the specimen was cooled down from deformation temperature under an applied load of 450 MPa to preserve the final dislocation structure. The change of the  $\gamma'$  precipitate shape was characterised by SEM in specimens crept at 850 °C and 900 °C with loads of 460 MPa and 275 MPa, respectively. These tests were terminated after about 3% of plastic elongation. More details about the creep tests and creep strength of the material can be found in [8]. The specimens for TEM investigations were cut perpendicular and parallel to the external stress axis. These specimens were ground to a thickness below 100  $\mu\text{m}$  and subsequently thinned to electron transparency by twin jet polishing using an agent of perchloric acid and butanol. A Philips CM200 was used to perform the TEM investigations. To interpret the development of the dislocation structure during creep the lattice mismatch in an undeformed specimen was determined at room temperature, 850 °C and 900 °C. This was done by high energy X-ray diffraction at the High Energy Materials Science (HEMS) beamline of the Helmholtz-Zentrum Geesthacht at the PETRA III storage ring of DESY in Hamburg, Germany. A specimen with a diameter of 4 mm was measured in transmission geometry with a photon energy of 87 keV ( $\lambda = 0.1425 \text{ \AA}$ ). The resulting reflections were recorded on a Mar345 image plate detector. For heating a specimen environment with an induction furnace was used and the specimen was under argon atmosphere during the measurement. The temperature was controlled by thermocouple directly spot-welded onto the specimen. More details about this specimen environment are published elsewhere [15]. The (002) peaks were recorded, which are a combination of the sub-peaks of the  $\gamma$ - and  $\gamma'$ -phase. By fitting the respective sub-peaks to the overall shape of the (002) peak using Pseudo Voigt functions the lattice constants of the

phases  $\gamma$  and  $\gamma'$  could be determined. For peak fitting the software package XPLOT (ESRF) was used and after providing starting parameters for two sub-peaks manually the fitting procedure was performed automatically by the program. A separation into three sub peaks was discarded as the difference in lattice misfit between a fit with two or three sub peaks was found to be negligible. From the lattice constants of the phases  $\gamma$  and  $\gamma'$ ,  $a_\gamma$  and  $a_{\gamma'}$ , the lattice mismatch  $\delta$  was calculated by the following formula:  $\delta = 2(a_{\gamma'} - a_\gamma)/(a_\gamma + a_{\gamma'})$ . By recording a number of profiles at the same temperature the standard deviation for lattice mismatch measurements was determined to be in the range of  $\pm 0.01$  % in these experiments.

### Results and Discussion

Figure 1 shows the microstructure of the alloy Co-9Al-9W-0.1B pictured by SEM in the undeformed state (figure 1 a), after creep deformation at 850 °C (figure 1 b) and after creep deformation at 900 °C (figure 1 c). While the as-received state exhibits cuboidal  $\gamma'$  precipitates with an edge length between 200 to 300 nm the precipitates in the crept specimens are directionally coarsened. Their preferential orientation is perpendicular to the externally applied compressive stress. This directional coarsening is especially pronounced for the specimen crept at 900 °C (figure 1 c). In accordance to Nabarro [13] this coarsening perpendicular to the applied external compressive stress hints to a positive lattice mismatch of the alloy. Directional coarsening with a preferential orientation which could be explained as an effect of a positive lattice mismatch was also observed by Titus et al. [9] in similar Co-base alloys. It is interesting to note that secondary  $\gamma'$  particles are found in the  $\gamma$  channels of the specimen crept at 900 °C (figure 1c). Most probably at the temperature of 900 °C, which is roughly 50 K below the  $\gamma'$  solvus of the alloy, a significant amount of  $\gamma'$  phase was already dissolved during the creep test and reprecipitated again as secondary  $\gamma'$  particles when the specimen was cooled down after the creep test.

To confirm that the lattice mismatch of the Co-9Al-9W-0.1B alloy under investigation here is positive the lattice mismatch was determined by X-ray diffraction. This was done between room temperature and 900 °C. It is known from Ni-base superalloys that the mismatch changes significantly with increasing temperature. This is a combined effect of the different thermal expansion coefficients of the phases  $\gamma$  and  $\gamma'$  and the redistribution of alloying elements between the  $\gamma$ - and the  $\gamma'$ -phase at higher temperatures [16,17]. For this reason some Ni-base superalloys which have a positive mismatch at room temperature nevertheless have a negative mismatch above ca. 750 °C (e.g. [18]). Therefore it was not only examined by high energy X-ray diffraction if the mismatch in the Co-base superalloy under investigation here is positive at room temperature in accordance with Sato's results [1] but also if it remains positive at the temperature of the creep experiments. At room temperature the lattice constants with 0.3581 nm for the  $\gamma$  matrix and 0.3609 nm for the  $\gamma'$  phase are in good agreement with the values given by Sato et al. [1]. This results in a positive lattice mismatch of 0.8 %. With increasing temperature the amount of mismatch decreases, but to such a low extent that it is still positive with 0.35 % at 850 °C and 0.1 % at 900 °C. The corresponding lattice constants of the phases  $\gamma$  and  $\gamma'$  at 850 °C are 0.3645 nm and 0.3658 nm, respectively. At 900 °C a lattice constant of 0.3656 nm is determined for the  $\gamma$  phase and of 0.3658 nm for the  $\gamma'$  phase. Three corresponding X-ray peaks for room temperature, 850 °C and 900 °C are shown in figure 2.

So it is evident that the Co-9Al-9W-0.1B alloy not only exhibits a positive lattice mismatch at the temperatures of the creep experiments but also the predictions of Nabarro [13] that directional coarsening perpendicular to the external compressive stress axis will occur under such conditions are confirmed experimentally.

Figure 3 shows the dislocation structure imaged under two-beam condition using a (200) reflection in a specimen crept at 850 °C with an applied load of 450 MPa (creep strain ca. 2 %) [10]. The TEM foil is perpendicular to the stress axis which itself is nearly parallel to the [001] direction of the grain pictured here. Straight dislocation segments in the horizontal matrix channels running inclined by 45° relative to the  $\gamma'$ -cubes are clearly discernible. Two directions of dislocations are visible, which lie under 90° relative to each other. Stacking faults, which extend over a number of  $\gamma'$ -particles and the matrix channels between them, are another feature of the deformation structure (marked by arrows in figure 3). Dislocations in slip configuration under compressive creep can either operate on the  $\langle 011 \rangle \{111\}$  or  $\langle 101 \rangle \{111\}$  slip system in a grain with its [001] orientation nearly parallel to the external compressive stress axis. This is the configuration investigated here. An analysis of the Burgers vector in one grain using the  $\vec{g} \cdot \vec{b}$  extinction criterion revealed that the dislocations indeed were predominantly of  $b = \pm a/2[011]$  matrix type. This is one of the slip systems expected to be active in the  $\gamma$ -matrix under the applied deformation conditions. This is illustrated in figure 4 where the same specimen position is shown using a (020) in one case (left) and a (200) two beam condition in the other (right). All dislocation segments are visible in the (020) condition as expected for  $b = \pm a/2[011]$ . On the contrary the majority of dislocation segments are out of contrast for the (200) two beam condition. That a weak residual contrast is still visible is due to the fact that the dislocation segments deposited at the

$\gamma/\gamma'$  interface have no pure screw but a mixed screw-edge character. That one slip system was activated predominantly may be due to a slight misalignment of the [001] orientation of the grain under investigation and the externally applied stress.

It is interesting to note that many stacking faults not only exist in the  $\gamma'$  precipitates but some also extend over the matrix channels. An example is shown in more detail in figure 5 at the position marked with A. This is different from the structures reported after compressive tests by Suzuki et al. [6,7] where pronounced stacking fault activity was only observed in alloys where Ta was added while bypassing of  $\gamma'$  precipitates by ordinary dislocations was the dominant mechanism in a ternary Co-Al-W alloy at 900 °C. With the limited amount of data available now, one can only speculate why significant stacking fault activity during creep is also present in the ternary Co-Al-W alloy under investigation here in contrast to the findings of Suzuki et al. for similar ternary Co-base alloys in compressive testing [7]. In this respect it is interesting to note that also Huis in't Veld et al. [19] reported stacking faults initially contained in the interior of  $\gamma'$  particles to extend into the matrix in later stages of deformation in Ni-base superalloys. Stacking faults in the precipitates as well as in the matrix in crept specimens were also observed by Gu et al. [20]. But the alloys investigated by them, besides having a high Co-content, were nevertheless Ni-based and also the creep temperature in their work with 725 °C was lower than in this study. Therefore, it seems that the occurrence of stacking faults and  $\gamma'$  cutting is associated with creep in the ternary Co-Al-W alloys, while bypassing of  $\gamma'$  precipitates is the favoured mechanism under higher loads and strain rates as encountered in compressive testing. Also it can be concluded that cutting of  $\gamma'$  precipitates by partial dislocations generating a stacking fault, which is a deformation mechanism in Ni-base superalloys at lower temperatures during creep, does occur more easily in these L1<sub>2</sub> hardened Co-base alloys at higher temperatures.

Figure 6 illustrates the dislocation structure in more detail. Dislocations either cross each other without any visible interaction resulting in a cube shaped pattern (see position A in figure 6) or form a more wavy structure (see positions B in figure 6). In this wavy structure dislocations form 90° angles which are more or less rounded at the corner tip. In Ni-base superalloys under low to medium stress high temperature conditions similar dislocation structures were reported by Field et al. [21]. These dislocation structures represent different early stages during the build up of interfacial dislocation networks at the  $\gamma/\gamma'$ -interfaces and are observed in Ni-base superalloys under low stress / high temperature conditions. For the Co-base alloy under investigation here creep at 850 °C is also in the high temperature range, since it is approximately 100 K below the  $\gamma'$  solvus temperature [8] and well above the temperature of the anomalous shear stress maximum reported by Suzuki et al. for these ternary Co-base alloys [6,7]. Therefore, we can try to interpret the observed dislocation structures based on the mechanisms which play a role during creep in Ni-base superalloys. Dislocation slip is first activated in the matrix channels and most of the dislocations do not penetrate into the  $\gamma'$ -precipitates but leave a dislocation segment with a  $\langle 110 \rangle$  line direction and a mixed screw-edge character at the matrix particle interface. The deposition of matrix dislocations at the  $\gamma/\gamma'$  interfaces is most probably due to the high deformation resistance of the ordered L1<sub>2</sub>  $\gamma'$  phase against shear by ordinary matrix dislocations compared with the softer matrix. Dislocations with the same  $\langle 011 \rangle$  or  $\langle 101 \rangle$  Burgers vector can operate on two different {111} slip planes. Therefore, dislocations with same burgers vector operating on two {111} planes can form the pattern of dislocation lines intersecting under 90° when deposited at the precipitate-matrix interface which are shown in figure 6. By reaction of these dislocations at the intersection points the 90° angles with rounded tips develop which are marked as B in figure 6.

It was predicted by Nabarro [13] that during the first stage of creep the dislocation activity is contained in one family of matrix channels either parallel (vertical) or perpendicular (horizontal) to the external applied stress. Which orientation of channels is preferred depends on the mode of creep deformation either compressive or tensile and the sign of the lattice mismatch between the phases  $\gamma$  and  $\gamma'$  [13]. A penetration of dislocations into the other orientation of matrix channels does not occur in this initial stage of creep. This leads to the extended horizontal dislocation arrangements observed in figures 3 and 5. For comparison figure 7 shows a micrograph from a TEM foil prepared parallel to the external stress axis. The deformation conditions in the grain under investigation are similar to the ones in figure 3, 4 and 5, i.e. [001] direction of the grain nearly parallel to the external stress axis, while the foil normal is oriented near the [100] direction. It is evident that the dislocation activity in the matrix channels parallel to the external stress axis is much less pronounced compared to the horizontal matrix channels shown in figure 6. While few dislocations are visible in figure 7 nevertheless two stacking fault ribbons are observed which are associated with the cutting of a number of  $\gamma'$  precipitates. In some cases the stacking fault extends over the  $\gamma$  matrix channel between two neighbouring  $\gamma'$  precipitates.

It is interesting to note that dislocations not only stop at the  $\gamma/\gamma'$  interfaces in horizontal matrix channels but also do not penetrate in adjacent vertical matrix channels. In figure 5 it is shown at the position marked with B that the

penetration of parallel matrix channels by dislocation is just beginning. That ordinary matrix dislocations operate predominantly in the horizontal matrix channels, do not easily penetrate into vertical matrix channels as shown in figure 5 and that the dislocation activity in vertical channels is less pronounced as shown in figure 7 can be understood by the different local stress states in both orientations of matrix channels in accordance with Nabarro's predictions [13]. For compressive creep stress and a positive lattice mismatch (i.e.  $\sigma\delta < 0$ ) the coherency stresses in the vertical  $\gamma$  channels reduce the local stress state in these channels. Therefore dislocation segments bowing out from horizontal matrix channels into vertical parallel channels experience a reduced acting shear stress as soon as they penetrate into the vertical channel. This is exactly the situation observed here. Also due to this reduced acting stress in the vertical matrix channels the amount of dislocations generated and operating there is lower than in the horizontal matrix channels.

So while at first sight microstructural features in these crept Co-base alloys are rather similar to Ni-base superalloys due to the positive lattice mismatch at creep temperature the dislocation activity starts in the other orientation of matrix channels. Another difference is the observation of precipitate cutting by partial dislocations associated with stacking faults. In Ni-base alloys under high temperature / low stress conditions precipitates are usually cut pairwise by ordinary dislocations connected by a antiphase boundary (APB). It is noteworthy that a dislocation configuration, which is similar to the one typical for the initial stages of creep in Ni-base superalloys, is found at a creep strain as high as nearly 2 %, i.e. well after the creep minimum, in this Co-base superalloy. The reason that fully developed interfacial dislocation networks built so slowly in the specimens under investigation is not understood yet. Nevertheless, such good microstructure stability may be beneficial for the application of these Co-base superalloys as structural high temperature material.

The positive lattice mismatch exhibited by these novel Co-base superalloys at creep temperature is also interesting with respect to creep strength. There are hints in literature [22] that a positive lattice mismatch may be advantageous for creep strength but no Ni-base superalloys with reasonable creep strength and a positive mismatch at higher temperatures exist to proof this concept or benefit from it. In this respect Co-base superalloys could be considered as model material to further investigate if a positive mismatch at creep temperature is really advantageous as well as materials which could benefit from this effect.

### *Conclusions*

The deformation structures found in ternary Co-W-Al superalloys hardened by a  $L1_2$  precipitate phase are in many respects similar to the ones found in Ni-base superalloys under similar conditions. Dislocation activity starts in one orientation of matrix channels while  $\gamma'$  precipitates are not sheared by these ordinary matrix dislocations. The dislocations in matrix channels are of the  $a/2\langle 101 \rangle\{111\}$  type. Nevertheless, there are also significant differences. Rafting perpendicular to the external stress axis in compressive creep is observed while most Ni-base superalloys raft parallel under comparable conditions. Also the dislocation activity is initially confined to matrix channels perpendicular to the stress axis instead of parallel channels as in Ni-base superalloys. These are effects of the positive lattice mismatch of this alloy at creep temperature. This strong preference for dislocation activity in one orientation of matrix channels is still present after the specimen experienced significant plastic deformation of up to 2 %. These observations are in good accordance with the predictions in literature [13,22] for positive mismatch alloys. Shearing of  $\gamma'$  precipitates is associated with stacking faults which frequently extend over matrix channels and neighbouring  $\gamma'$  particles.

### *References*

- [1] J. Sato, T. Omori, K. Oikawa, I. Ohnuma, R. Kainuma, K. Ishida, Science 312 (2006) 90-91.
- [2] A.M. Beltran, in: C.T. Sims et al. (Eds.), Superalloys II, Wiley, New York, 1987, pp. 135-163.
- [3] T.C. Du Mond, P.A. Tully, K. Wikle, Ninth ed. Metals Handbook, vol. 3, American Society for Metals, Metals Park, OH, 1980, pp. 589-594.
- [4] T.M. Pollock, J. Dibbern, M. Tsunekane, J. Zhu, A. Suzuki, JOM 62 (2010) 58-63.
- [5] M. Tsunekane, A. Suzuki, T.M. Pollock, Intermetallics 19 (2011) 636-643.
- [6] A. Suzuki, G.C. DeNolf, T.M. Pollock, Scr. Mater. 56 (2007) 385-388.
- [7] A. Suzuki, T.M. Pollock, Acta Mater. 56 (2008) 1288-1297.
- [8] A. Bauer, S. Neumeier, F. Pyczak, M. Göken, Scr. Mater. 63 (2010) 1197-1200.
- [9] M.S. Titus, A. Suzuki, T.M. Pollock, Scr. Mater. 66 (2012) 574-577.
- [10] A. Bauer, S. Neumeier, F. Pyczak, R.F. Singer, M. Göken, Mater. Sci. Eng. A550 (2012) 333-341.

- [11] M.S. Titus, A. Suzuki, T.M. Pollock, in: E.S. Huron et al. (Eds.), 12th Int. Symposium on Superalloys, The Minerals, Metals and Materials Society, Warrendale PA, 2012, pp. 823-832.
- [12] A. Bauer, S. Neumeier, F. Pyczak, R.F. Singer, M. Göken, in: E.S. Huron et al. (Eds.), 12th Int. Symposium on Superalloys, The Metallurgical Society of AIME, Warrendale, PA, 2012, pp. 695-703.
- [13] F.R.N. Nabarro, *Metall. Mater. Trans.* 27A (1996) 513-530.
- [14] K. Shinagawa, T. Omori, K. Oikawa, R. Kainuma, K. Ishida, *Scr. Mater.* 61 (2009) 612–615.
- [15] A. Stark, M. Oehring, F. Pyczak, A. Schreyer, *Adv. Eng. Mater.* 13 (2011) 700-704.
- [16] Y.N. Gornostyrev, O.Y. Kontsevoi, K.Y. Khromov, M.I. Katsnelson, A.J. Freeman, *Scr. Mater.* 56 (2007) 81–84.
- [17] F. Pyczak, S. Neumeier, M. Göken, *Mater. Sci. Eng. A* 527 (2010) 7939-7943.
- [18] F. Pyczak, B. Devrient, H. Mughrabi, in: K.A. Green et al. (Eds.), 10th Int. Symposium on Superalloys, The Metallurgical Society of AIME, Warrendale, PA, 2004, pp. 827-836.
- [19] A.J. Huis in't Veld, G. Boom, P.M. Bronsveld, J.Th.M. De Hosson, *Scr. Met.* 19 (1985) 1123-1128.
- [20] Y.F. Gu, C. Cui, D. Ping, H. Harada, T. Fukuda, J. Fujioka, *Mater. Sci. Eng. A* 510-511 (2009) 250-255.
- [21] R.D. Field, T.M. Pollock, W.H. Murphy, in: S.D. Antolovich et al. (Eds.), 7th Int. Symposium on Superalloys, The Metallurgical Society of AIME, Warrendale, PA, 1992, pp. 557-566.
- [22] H. Mughrabi, U. Tetzlaff, *Adv. Eng. Mater.* 2 (2000) 319-326.

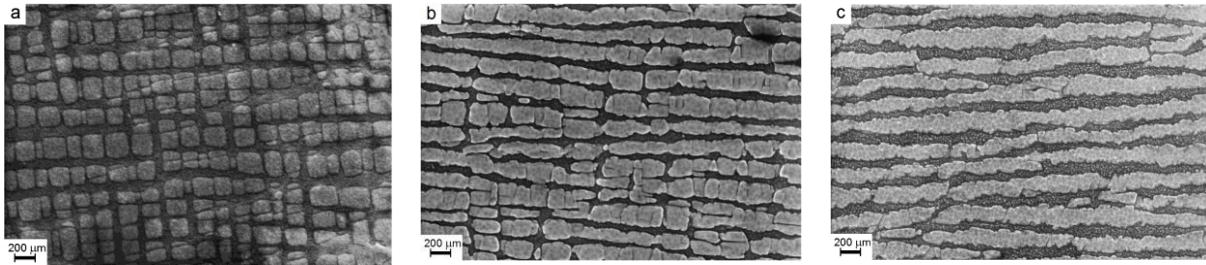


Figure 1: SEM micrographs of the undeformed state (a), a specimen crept at 850 °C (b) and a specimen crept at 900 °C (c); the external stress axis is vertical in b and c.

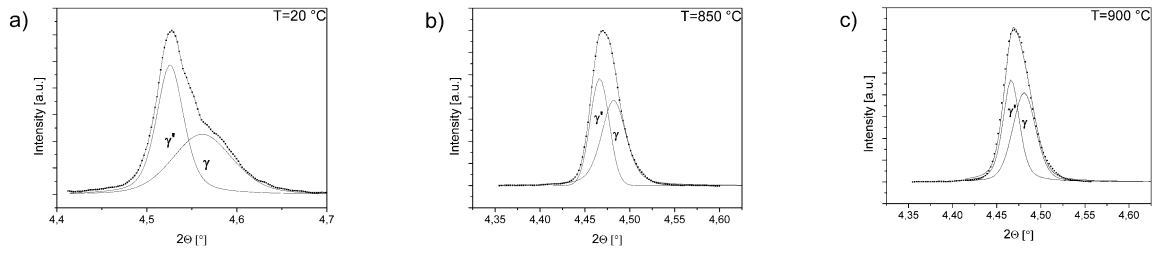


Figure 2: (002) diffraction peaks of an undeformed specimen recorded at 20 °C (a), 850 °C (b) and 900 °C (c); the fitted sub-peaks of the phases  $\gamma$  and  $\gamma'$  are also shown in the plots.

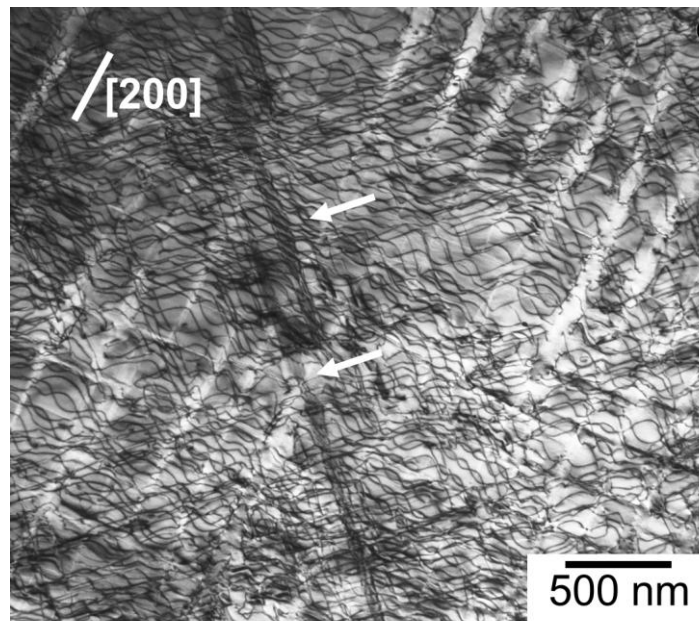


Figure 3: Crept specimen (850 °C, TEM foil perpendicular to external stress axis) imaged with beam direction near [001] using a (200) reflection in a two beam condition; wavy dislocation structures and extended stacking faults (arrows) are visible in the specimen (after [10]).



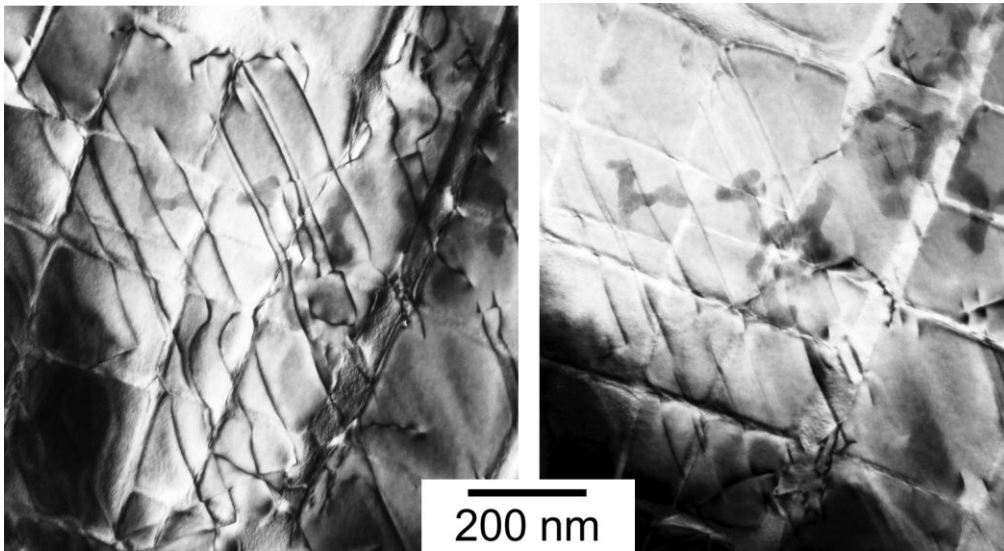


Figure 4: Dislocation structure pictured using a (020) (left) and a (200) (right) two beam condition in specimen crept at 850 °C..

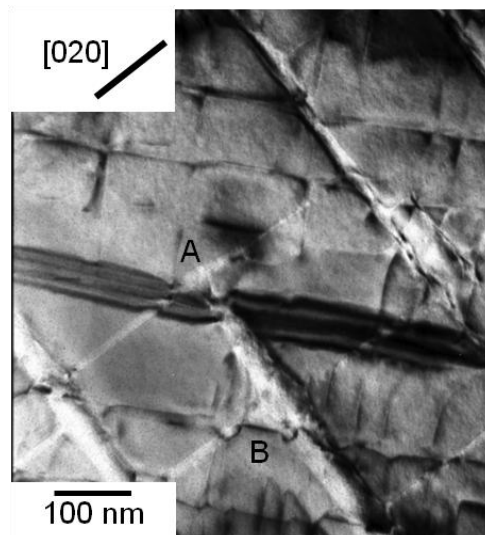


Figure 5: Stacking fault extending over  $\gamma'$ -precipitates and matrix channel (marked A) and dislocation segments starting to penetrate into parallel matrix channels (marked B); beam direction near [001] using a (020) reflection in specimen crept at 850 °C.

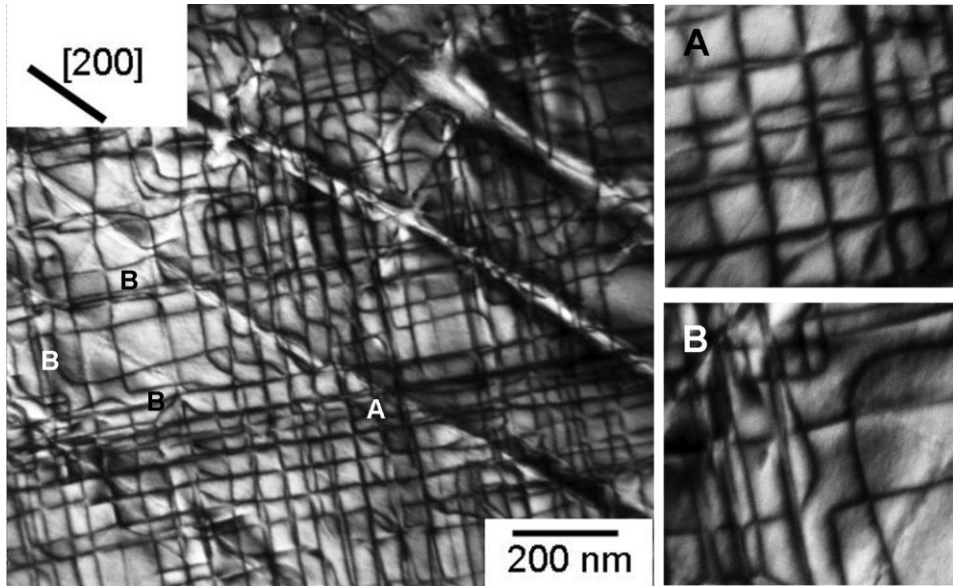


Figure 6: Dislocation structure imaged with beam direction near  $[001]$  using a  $(200)$  reflection; straight dislocations forming a cube pattern (marked A) and dislocation reactions at intersection points are visible (marked B) in specimen crept at  $850\text{ }^{\circ}\text{C}$  (left); enlarged examples of dislocation intersections (A) and dislocation reactions (B) are shown enlarged (right top and bottom).

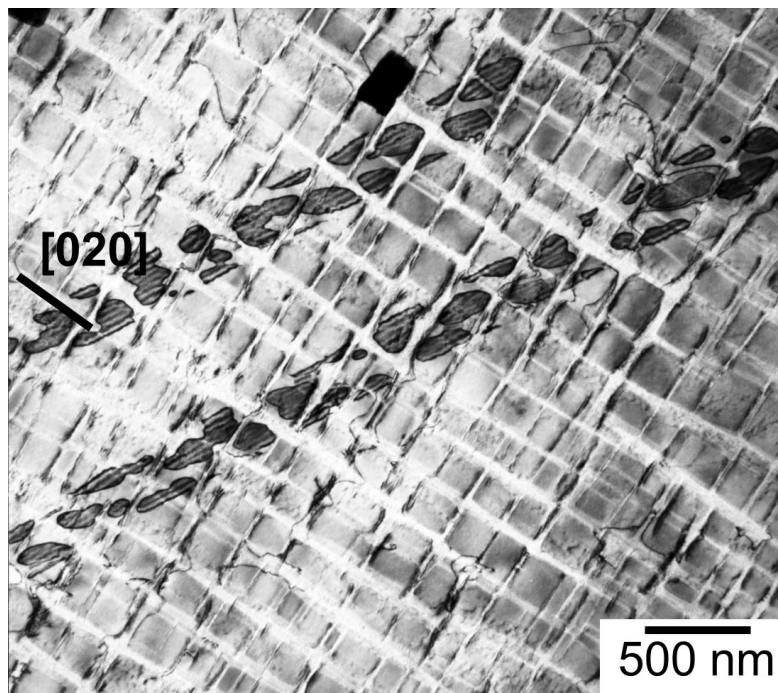


Figure 7: Crept specimen (TEM foil parallel to external stress axis) imaged with beam direction near  $[100]$  using a  $(020)$  reflection in a two beam condition; few dislocations are visible while two bands of stacking fault ribbons are observed in the  $\gamma'$  precipitates which in some positions also span over the matrix channels in specimen crept at  $850\text{ }^{\circ}\text{C}$ .